Journal of Catalysis **198,** 164–171 (2001)
doi:10.1006/jcat.2000.3072, available online at http://www.idealibrary.com on IDEAL®

Deep Oxidation of Methane on Alumina–Manganese and Pt-Containing Catalysts

P. G. Tsyrulnikov,*,[1] V. S. Sal'nikov,* V. A. Drozdov,* A. S. Noskov,† N. A. Chumakova,† V. K. Ermolaev,† and I. V. Malakhova†

Omsk Department of the Boreskov Institute of Catalysis SB RAS, Neftezavodskaya 54, 644040 Omsk, Russia; and †Boreskov Institute of Catalysis SB RAS, Pr. Akad. Lavrentieva 5, 630090 Novosibirsk, Russia

Received November 30, 1999; revised September 14, 2000; accepted September 18, 2000; published online February 13, 2001

The kinetics of deep methane oxidation was studied over a manganese–alumina catalyst and a reference catalyst—a tableted mechanical mixture of 2% Pt + γ-Al_2O_3. The reaction temperature ranged from 400 to 800°C, the methane concentration was up to 4.5 vol%, and the oxygen content was up to stoichiometry. The higher the catalyst activity, the lower the probability for the homogeneous continuation of the catalytic reaction to proceed, even at 800°C with the stoichiometry gas mixture composition. The distance over which alkyl peroxide catalysts escape from the catalyst surface under reaction conditions was estimated.

Key Words: **catalyst; manganese oxides; platinum; methane; deep oxidation.**

INTRODUCTION

It has been shown (1) that when lean gas mixtures are burnt according to reverse-process technology (2), one may accumulate heat in the reactor at rather high temperatures and then successfully recover it. In this case it is necessary to use catalysts which resist high temperatures well. Therefore, we started to develop combustion catalysts which resist high temperatures up to 1000°C. At present the best catalyst is registered as IC-12-40 and is commercially produced by Katalizator Company, Ltd., in Novosibirsk, Russia. In the United States it is known as Z-2 (3).

This catalyst was tested in reverse-process technology for burning a mixture of 1.5 vol% *n*-butane balance air (4). After the catalyst temperature reached 700°C and the heat front came to the inert part of the bed (ceramic Rachigue rings), then, as the gas flow direction was switched to the opposite way, the oxidation reaction continued in the inert bed, and the reaction temperature increased to 1090°C. The heat front, propagating back through the catalyst bed, partially involved the ceramic rings in methane oxidation (Fig. 1). Therefore, a homogeneous oxidation reaction might develop in the inert bed, initiated by some radical species produced in the process of heterogeneous catalytic oxidation.

Since the catalytic combustion of methane from the vent gases of coal mines is one of the most promising ways to use reverse-process technology, it has been important to study the kinetics of methane combustion over the heat-resistant catalyst IC-12-40 in a wide range of temperatures and methane concentrations and to estimate the contribution of homogeneous reactions in the oxidation process rate. We intend to use the obtained data for process modeling to optimize catalyst grain geometry.

EXPERIMENTAL CONDITIONS

1. Catalysts

A lab scale sample of supported alumina–manganese catalyst IC-12-40 was prepared. γ-Alumina extrudates, obtained from pseudoboehmite peptized by nitric acid, hydrated, and then thermally activated, was exposed to incipient wetness impregnation by the manganese nitrate solution. After impregnation the sample was dried at 120°C for 4 h, calcined at 700°C for 3 h, and thermally activated at 970°C for 4 h. The manganese concentration in the thus-obtained catalyst was 12 wt%, as refers to MnO_2. Catalyst features are discussed elsewhere (5–10).

Two more catalysts were also studied in methane oxidation. One was a pelletized mechanical mixture, Pt black + γ-alumina, containing 2 wt% Pt. Another catalyst was Pt, supported on a cordierite honeycomb monolith washcoated with γ-alumina and containing 0.2 wt% Pt.

2. Kinetic Measurements

Kinetic studies were done using a gradientless flow curcuit setup. This setup consisted of a unit for gas mixture preparation and supply, a chromatography analysis unit, and a circuit made of a glass or quartz reactor with a coiled heat exchanger and a membrane circulation pump. The

[1] To whom correspondence should be addressed. Fax: +7-381-2-646156. E-mail: tsyr@incat.okno.ru.

0021-9517/01 $35.00

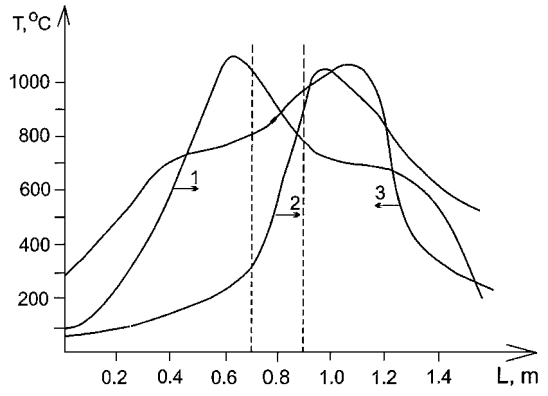

FIG. 1. Temperature profiles in the reverse-flow reactor after flow reversal (see Drozdov *et al.* (4)) in $t = 20$ (1), 55 (2), and 35 min (3). Arrows show the gas flow direction. The catalyst bed is placed between 0.7 and 0.9 m; the remaining parts are filled with inert ceramic Rashig rings.

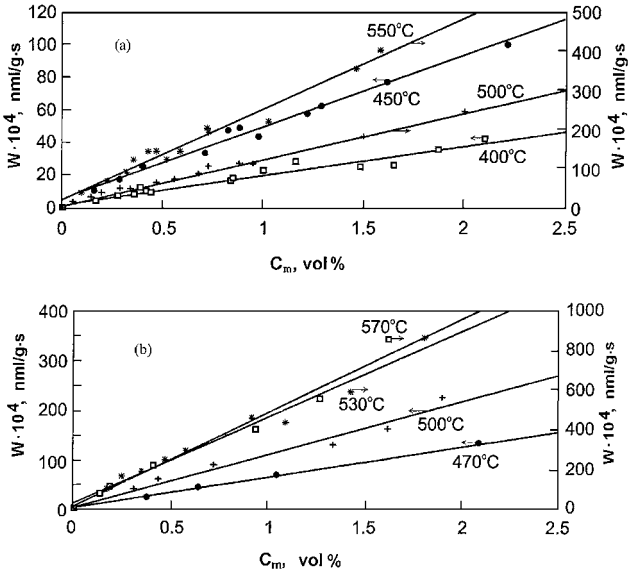

FIG. 2. Activity of the Al–Mn catalyst versus methane concentration: (a) catalyst grain size is 4 mm; (b) catalyst fraction of 0.4–0.8 mm.

latter pumped the gas mixture through reactor in one direction and is guided by a special electric–pneumatic system, allowing a capacity ranging from 100 to 1300 L/h. An air rotameter inserted in the circuit was used to calibrate the pump at room temperature.

The reactor with the heat exchanger was put into the gradientless furnace, while the remaining part of the circuit was installed in a thermostat. The thermostat temperature could rise to 250°C. The exchanger efficiently heated the gas mixture to the required temperature, which at the reactor inlet was measured with a Chromel–Alumel thermocouple. The outlet gas flow was cooled in steel capillaries.

Temperature below 600°C. A flow circuit setup with a glass tube reactor (inner diameter 16 mm) was installed into a gradientless furnace. The gas flow rate varied within 4–50 L/h, and the circulation rate was 800 L/h. The inlet methane concentration in air varied within 0.2–2.5 vol%. Alumina–manganese catalyst extrudates were 4 mm in diameter and 4–5 mm long. Smaller particles 0.4–0.8 mm in size were prepared from the same catalyst. The catalyst temperature was measured with a Chromel–Alumel thermocouple installed in the catalyst bed.

Temperature up to 850°C. A quartz reactor (inner diameter 15 mm) with a quartz filter at its bottom was put into the gradientless furnace and operated with inner circulation. The distance between the gas inlet and the filter was 45 mm. The temperature was measured by a thermocouple inserted into a thin quartz housing over the catalyst bed. The circulation rate varied from 300 to 1300 L/h, and the gas flow varied from 4 to 65 L/h. The inlet methane concentration in air varied from 0.4 to 4.5 vol%. The granulometry of catalyst IC-12-40 was exactly as described in the previous paragraph.

RESULTS AND DISCUSSION

Temperature Interval 400–600°C

Experiments performed in the empty reactor (either glass or quartz) prove that at studied temperatures no oxidation occurs independent of the methane concentration in air.

Catalytic oxidation kinetics obtained at temperatures below 600°C are presented in Figs. 2 and 3. Comparing the performance of large and small catalyst grains, we may see that below 500°C there is no difference in reaction rates. Therefore, even on large grains oxidation proceeds in the kinetic region. Nevertheless, function lg W versus $1/T$ shows the inner diffusion limitation in the larger grains starting at temperatures above 500°C. Indeed, the activation energy for small grains at 470–600°C is 25–26 kcal/mol, while for the large grains it is 18 kcal/mol. We may represent the kinetic equation as follows.

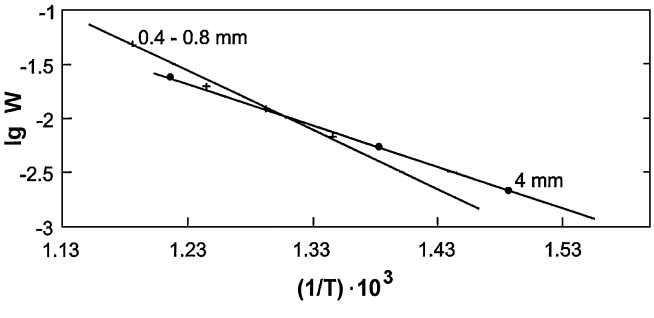

FIG. 3. Arrhenius plot for the Al–Mn catalyst.

Whole large grains.

$$W = 1.38 \cdot 10^5 \cdot \exp(-18{,}000/R \cdot T) C_m,$$

$$(n\text{ml } CH_4 \text{ reacted})/g \cdot s,$$

where W is the reaction rate, $E_a = 18{,}000$ cal/mol is the apparent activation energy, the reaction rate constant at 500°C is 1.12 L/g · s, and C_m is the current methane concentration in air, ($n$ml CH_4)/(L gas mixture), where "$n$ml CH_4" means milliliters of CH_4 reacted at STP (273 K and 0.1 MPa).

Crushed small grains.

$$W = 1.91 \cdot 10^7 \cdot \exp(-25{,}500/R \cdot T) C_m,$$

$$(n\text{ml } CH_4 \text{ reacted})/g \cdot s,$$

where 1.18 L/g · s is the oxidation rate constant at 500°C.

The maximum deviation of the experimental reaction rates from those estimated according to the kinetic equations does not exceed 20%.

According to the data presented in Fig. 3, at temperatures higher than 500°C on large grains the apparent activation energy is 18 kcal/mol, but not 13 kcal/mol, as follows from the theory. Note, however, that the Al–Mn catalyst is obtained via impregnation. Manganese nitrate sorbs poorly on γ-Al_2O_3. Upon drying a considerable amount of solution diffuses toward the grain surface. Therefore, there is a gradient of active component concentration in the ready catalyst grains. The active component concentration changes by 2.5- to 3-fold in going from the grain center to its surface. As a result we obtain the catalyst, which actually is not an eggshell catalyst with a thin crust. Moreover, the manganese nitrate solution is rather acidic (pH ~1). Since upon drying the grain surface is more heated than its center, pores near the surface increase owing to the partial dissolution and reprecipitation of Al_2O_3 caused by the solution acidity. We observed this phenomenon earlier (14), when we removed catalyst grain layers one by one in going from the surface inside the grain and studied the porous structure of these layers. Therefore, at high temperatures the grain periphery with large pores continues to work in the kinetic regime, while the grain center suffers from diffusion limitation. A superposition of these two processes at the grain surface and in the grain center provides a higher activation energy than is actually required under the inner diffusion regime.

Note that we observed no influence of reaction products (H_2O and CO_2) on the rate of deep methane oxidation over spent catalysts, which is in a good agreement with earlier results published elsewhere (11–13). Deep oxidation of paraffins is studied well enough. Thus in Refs. (11) and (12), paraffin oxidation was studied on the alumina–platinum catalyst AP-56 (0.56% Pt/γ-Al_2O_3), and the water content was varied in a large range. It has been shown that at temperatures above 220–250°C, water has no effect on the rate of oxidation of n-pentane, n-heptane, or n-nonane. Methane oxidation on the oxides of metals of Period 4 and on spinels (cobaltite, chromite, and ferrites) was studied in Ref. (13) and no effect of reaction products on the deep oxidation rate was noticed at 275–500°C, the reaction order being $n = 1$ with respect to the methane concentration and $n = 0$ with respect to the oxygen concentration.

In our experiments the inlet methane concentration in air was up to 4.5 vol%, and the methane conversion was higher than 50%. Although the water concentration twice exceeded that of methane, the reaction order with respect to methane was 1. Therefore, at temperatures starting from 400°C (most runs were done at 500–600°C and higher) water does not inhibit methane oxidation on the studied catalysts.

Temperature Interval 650–800°C

First, let us consider data obtained earlier on while studying methane oxidation in the empty reactor presented in Fig. 4. For simplicity we introduce relative units—logarithms of experimental reaction rates (in the whole reactor volume) and of the current methane concentrations divided by the minimum experimental rates and concentrations obtained at the given temperature. Apparently, at 700°C the reaction rate order with respect to the current methane concentration is about 1.2. As the reaction temperature increases, the reaction order increases up to 2.4–2.5, showing that some chain processes occur.

When the reaction performance in the empty reactor and the reactor filled with 1.6- to 2.5-mm quartz particles was compared, the gas flow rate ranged from 4 to 65 L/h. In the filled reactor residence time was twice as short at the same gas rate. However, if the gas flow rate in the filled reactor

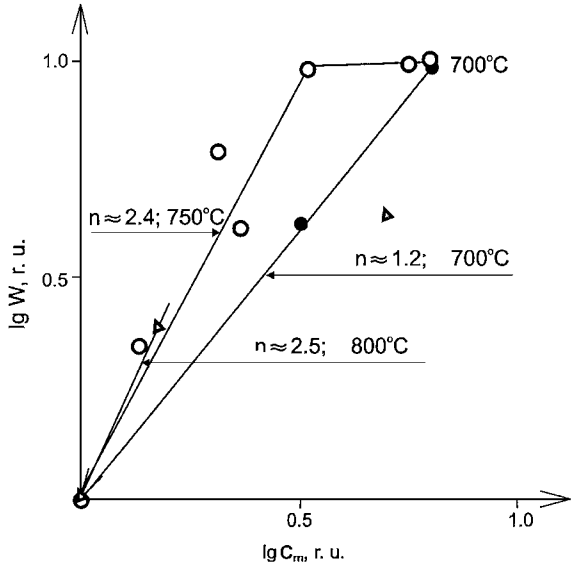

FIG. 4. lg W–lg C_m plot for the empty quartz reactor.

TABLE 1

Methane Conversion in the Empty Reactor Versus Circulation Rate

Circulation rate, Q, L/h	300	450	650	850	900
Conversion, X, %	52	40	29	19	17

Note. Flow rate, $V = 16$ L/h; inlet methane concentration, $C_0 = 2$ vol%; reaction temperature, $T = 750°C$.

was twice reduced, the residence time remained constant. Data processing shows that under these conditions methane conversion in the filled reactor remains similar to that attained in the empty reactor.

On one hand, this evidences that the quartz surface is inert in catalysis. On the other hand, we may not exclude surface chain reactions on the inert surface, since earlier we observed a sharp temperature increase in the bed of inert ceramic Rashig rings after the heat front propagation owing to the gas flow reversal (4).

Nevertheless, we may assume that in the empty reactor the reaction starts on the reactor walls and then transfers into the reactor bulk. Indeed, when we treat quartz reactor walls with H_2SO_4 solution (1 : 1) at 90°C for several hours, adding oxalic acid, methane conversion at 750°C in the empty reactor decreases by two- to three-fold (depending on the inlet methane concentration). Comparing these results with the data on methane oxidation over the IC-12-40 catalyst (see below) at temperatures above 700°C, we see that heterogeneous–homogeneous methane oxidation in the empty reactor has the following features:

(1) methane conversion decreases as circulation rate increases (Table 1);

(2) a nonidentified product appears at $T > 750°C$, which is most likely ethane or ethylene regarding the chromatography pattern.

Catalytic methane oxidation. Catalytic methane oxidation at high temperatures was performed with whole large catalyst grains. The catalyst sample weight varied from 0.1 (single grain) to 4.6 g. If other conditions were the same, up to 700°C the catalyst weight had no effect on the reaction rate per catalyst gram. Only at 750°C, with the catalyst weight being less than 0.3 g, did the reaction kinetics resembles that obtained in the empty reactor. The reaction rate begins to be dependent on the circulation rate, and the above-mentioned nonidentified product appears. Under other conditions the circulation rate has no effect on methane conversion, and there is no product of partial oxidation. The apparent reaction order is close to a unit (see Figs. 5 and 6 for the data obtained). Note that at all studied temperatures (450–750°C) the activation energy of methane oxidation on whole grains remains the same. Most likely, the contribution of oxidation inside the catalyst

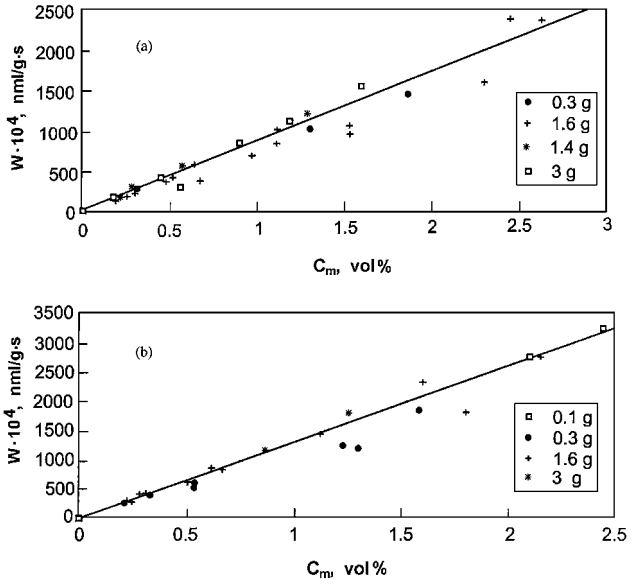

FIG. 5. The reaction rate versus methane concentration for various loads of Al–Mn catalyst, grain size 4 mm, temperature 650°C (a) and 700°C (b).

grains decreases as temperature increases. But this decrease is reimbursed by the contribution of the reaction proceeding in the subsurface crust of the grains, where most of the active component is concentrated. We observed a similar effect of a constant activation energy at 500–700°C when we performed methane oxidation on the grains of catalyst IC-12-1 (IC-12-40 analog) (15), which is copper oxide supported on γ-alumina extrudates (4–5 mm)×(6–8 mm) with a nonuniform distribution of active component.

Bed Dilution with Inert Particles

In order to reveal the homogeneous reaction contribution, experiments were done in a catalyst bed also loaded with inert spherical corundum (0.5–0.8 mm) or quartz (1.6–2.5 mm) trained at 900°C for 3 h. Inert particles filled the empty spaces between the catalyst grains. In addition, two inert 2-mm-thick beds were loaded under and over the catalyst bed, since we assumed that radicals forming in the catalyst bed were to be quenched in the inert beds.

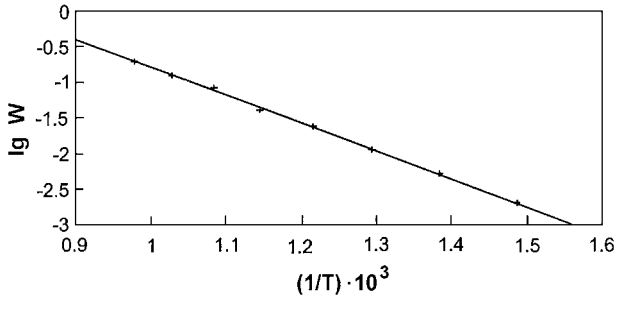

FIG. 6. Arrhenius plot for the Al–Mn catalyst, grain size 4 mm.

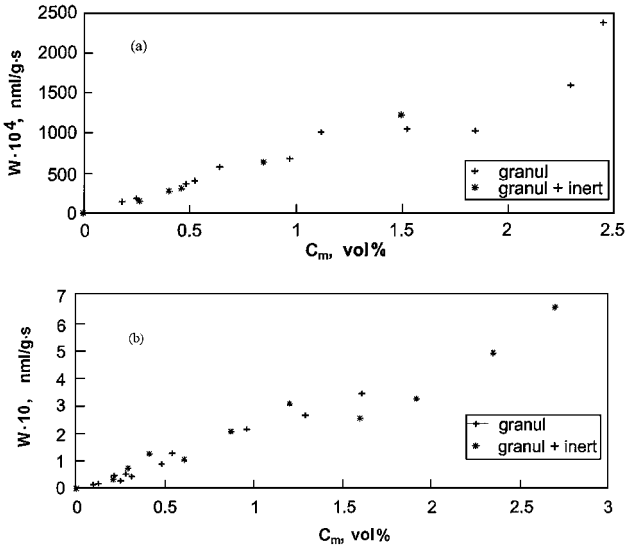

FIG. 7. The reaction rate versus methane concentration for the Al–Mn catalyst (grain size of 4 mm), with and without an inert quartz fraction (1.6–2.5 mm): (a) catalyst weight 1.6 g, temperature 650°C; (b) catalyst weight 0.3 g, temperature 750°C.

Experiments proceeded at temperatures ranging from 650 to 750°C (see Fig. 7). Apparently, catalyst dilution with inert particles had no effect on methane conversion. Therefore, we may conclude that no homogeneous reactions develops in the free space between the catalyst grains. Moreover, at the higher temperature (about 750°C) the catalyst added in small amounts into the empty reactor suppresses the oxidation process and essentially decreases methane conversion.

Experiments with Various Oxygen Content in the Gas Phase

1. Empty reactor. In these experiments the methane concentration ranged from 0.4 to 2.5 vol%. The oxygen content in the mixture with nitrogen varied from 2 to 21 vol%.

At oxidation in the empty reactor, as the oxygen content decreases methane conversion also decreases at the same inlet methane concentration. Thus, if the circulation rate is 900 L/h, the gas flow rate 8 L/h, temperature 750°C, and inlet methane concentration 2.2%, then the methane conversion decreases from 21 to 10% as the oxygen content decreases from 21 to 5%. At 800°C, flow rate 60 L/h, and initial methane concentration 0.46%, the same decrease in oxygen content results in a CH_4 conversion decrease from 42 to 8%.

At 750°C and the above-said conditions, in a reactor filled with quartz (1.6–2.5 mm), methane conversion decreases by 2–5% only. Most likely as the relative methane concentration increases, the methane molecule activation intensifies on the quartz surface, and chain reactions are initiated. This obstacle compensates for the decrease in methane conversion, which we observed without quartz, as the inlet oxygen concentration decreased.

2. Catalyst activity studies. Apparently (see Fig. 8, 600°C, inlet oxygen content 2 vol%), whole grains of IC-12-40 at first exhibit activity, which grows linearly as the current methane concentration increases. However, as the current methane concentration attains ~0.8 vol%, the catalyst activity becomes independent of the growing methane concentration. When the inlet oxygen content is 5 vol%, the catalyst activity becomes independent when the current methane concentration is about 1.7 vol%. At higher temperatures (see Fig. 8b, 650°C, inlet oxygen content 2 vol%), after its linear growth the catalyst activity stops increasing at $C_m \approx 1$ vol% and even starts to decrease.

The same results were obtained with the 0.4- to 0.8-mm grains of IC-12-40. No homogeneous reaction was registered under the studied conditions.

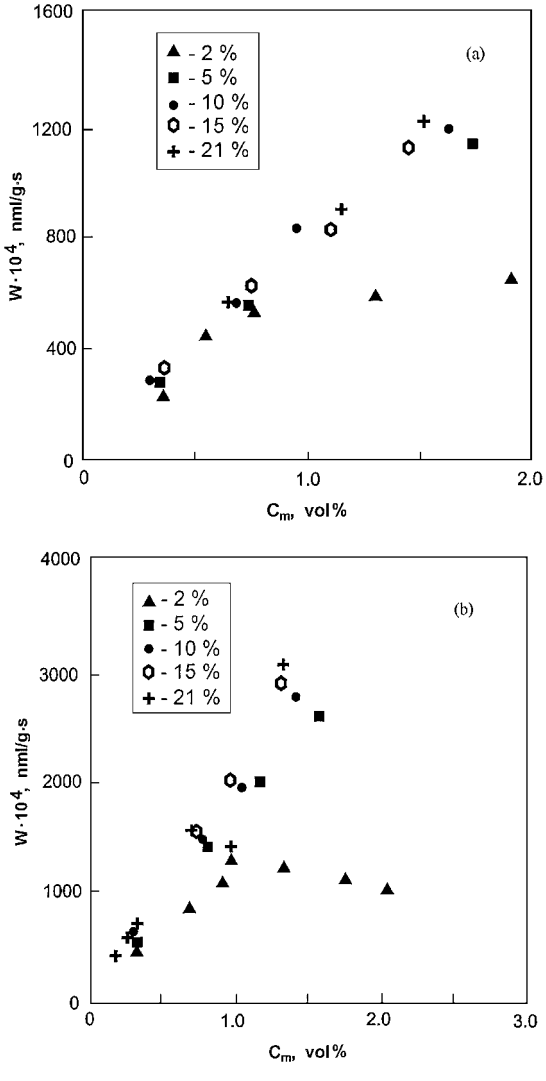

FIG. 8. The reaction rate versus current methane concentration at 600°C (a) and 650°C (b) at different inlet oxygen concentrations.

Platinum–Alumina Catalyst on a Cordierite Monolith

In order to understand whether the absence of a homogeneous reaction at catalytic methane oxidation is common, we tried a monolith platinum–alumina catalyst.

To stabilize catalyst performance, we calcined it at 750°C for 1 h in air. Two catalyst samples were prepared. One sample consisted of irregular pieces of crushed monolith walls. Another sample was a $8 \times 11 \times 6$ mm fragment cut out of monolith and loaded in the reactor with channels coaxial with the gas flow. Both samples were tested at 600–750°C at several methane concentrations. The specific activity (per 1 g of the catalyst) of irregular wall pieces was found not to differ from that of the monolith fragment. The order of the oxidation rate with respect to the methane concentration was close to a unit. Quartz filling had no effect on methane conversion (reaction rate) over both samples. Therefore, no homogeneous reaction proceeds during methane oxidation over a platinum–alumina catalyst.

Methane Oxidation on an Alumina-Manganese Catalyst Studied with the Matrix Isolation Method with EPR Spectra Recording

Methane oxidation on IC-12-40 was studied with a matrix isolation method accompanied by EPR spectra registration to obtain direct proof of the homogeneous reaction contribution. This method allows a direct observation of radical reaction products and their identification. The method is well described elsewhere (16).

Experiments were done using two catalysts: 2 wt% MnO_x/Al_2O_3 and 12wt% MnO_x/Al_2O_3, 3- to 5-mm fractions in both cases. The gas mixture (2.45% methane, 19.8% oxygen, balance nitrogen) was prepared in a cylinder. All gases were additionally dried (P_2O_5, silica KSK) and purified from admixtures (molecular sieves and distillation at liquid nitrogen temperature).

The reaction was performed in a flow vacuumed setup ($P < 10^{-2}$ Torr) using a quartz reactor (inner diameter 15 mm) with a grid for the catalyst. The latter was loaded with a single-grain-thickness layer. On the way to the freezing unit, before the first collision, desorbing radicals uptake the reactor wall temperature, which is room one (air blowing), so "radical hardening" takes place. Radicals, forming among the reaction products, were frozen at 77 K in the side arm of a Dewar vessel installed in the EPR resonator and connected to the flow vacuum system.

Experimental results showed accumulating alkyl peroxide radicals. Their EPR spectrum exhibited a single asymmetric singlet provided by the axial anisotropy of g-factor, $g_{\parallel} = 2.004$, and $g_{\perp} = 2.03$. In order to determine the radical concentration we used $CuCl_2 \cdot 2H_2O$ as a reference, with a radical concentration of $3.3 \cdot 10^{17}$. Radical registration, however, was poorly reproduced, most likely owing to the change in catalyst properties occurring at high temperatures (over 700°C) in a vacuum. Nevertheless, the formation of radicals $CH_3O_2^*$ was detected at 720°C, and the rate of their formation (estimated from the sample and reference intensities) was $6 \cdot 10^9$ radicals/s. We failed to register the CH_3 radical, which is the primary radical in the methane oxidation process. This may be caused by several reasons: (a) radical recombination on the reactor walls or catalyst surface; (b) its oxidation to CH_3O_2; (c) since we freeze products at liquid nitrogen temperature, we fail to stabilize them, owing to fast recombination in the condensate.

EPR spectra analysis of the catalysts before and after the reaction shows that the catalyst absorption line changes its width at the same intensity for both 2 and 12 wt% MnO_x content. Obviously, the catalyst active component changes its properties. Note that before the reaction the concentrations of catalyst paramagnetic centers differ by 50-fold ($3.1 \cdot 10^{19}$ for 2% and $1.41 \cdot 10^{21}$ for 12% MnO_x) and not by 6-fold, as might be expected according to the catalyst composition. This is quite understandable, since the relative degree of manganese–oxide interaction with alumina producing inactive EPR structures is far higher for the catalyst with a lower content of MnO_x.

Therefore, the reaction mechanism of deep methane oxidation indeed includes stages which produce active alkyl peroxide radicals. However, since the latter forms on the active catalyst surface at a high temperature, they are oxidized to CO_2 and H_2O before they are able to escape over a large distance into the gas phase. Some special conditions such as vacuum and flow regime allow their partial removal from the catalyst surface, freezing, and identification. This seems hardly probable under real conditions in the catalyst fixed bed.

Deep oxidation reactions on Al–Pt-catalysts studied with the EPR method are discussed in Ref. (16). It has been shown that at alcohol oxidation (and we may consider alcohols the primary products of paraffin oxidation) it is possible to identify only alkyl peroxide radicals that may be removed from the reaction zone for freezing owing to their low chemical activity. We probably fail to register hydroxyl radicals because they are rather active and may be oxidized in the gas phase to HO_2 radical, or they may be trapped by the support surface hydroxylating it.

Catalyst Pt–Al_2O_3 was not studied, since Pt^0 и Al_2O_3 show no EPR activity.

Synergy Effect for Deep Oxidation in the Pt Black + Alumina System

Experiments on the deep oxidation of alkanes done with the system concerned allow the estimation of a distance over which a radical particle may escape from the catalyst surface under real catalyst conditions. We found earlier (see (17, 18) and Fig. 9) that mechanical mixtures of platinum black with alumina or silica pelletized at a definite pressure show a significant synergy effect in the deep oxidation of

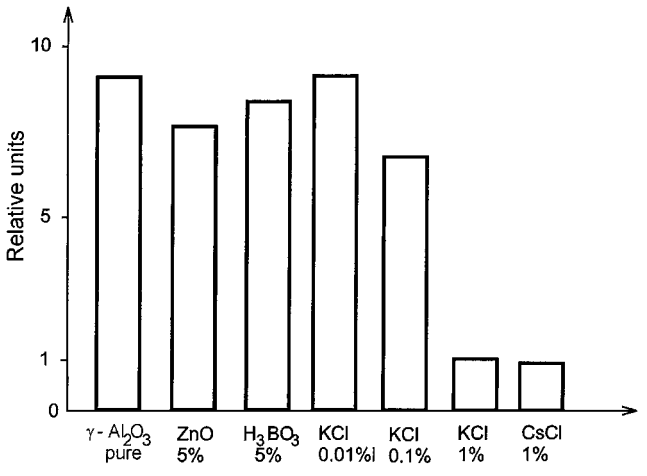

FIG. 9. Synergy effect at deep oxidation of n-C_4H_{10} on 2% Pt/γ-Al_2O_3 modified with radical traps.

butane and methane. Thus the activity per 1 g of black increases by an order of magnitude (by 8- to 12-fold), although pure oxides are not active under the reaction conditions (300 and 500°C, correspondingly). Let us consider our new data related to the deep oxidation of methane, presented in Fig. 10 in comparison with our previous results (17). Figure 10 shows the catalytic activity and porous structure of samples pressed into tablets depending on the tablet molding pressure. At a molding pressure of about 270 MPa, the volume of large pores (radius $r > 10$ nm, line 1 in Fig. 10) decreases almost to the minimum, while the volume of pores with $r < 10$ nm (line 2 in Fig. 10) is still equal to its starting value of 0.5 cm^3/g. This size ($r \approx 10$ nm) corresponds to the average distance between the particles of Al_2O_3 and Pt–Al_2O_3 in the catalyst (obtained at 270 MPa). In deep butane oxidation, activity per Pt gram attains its maximum

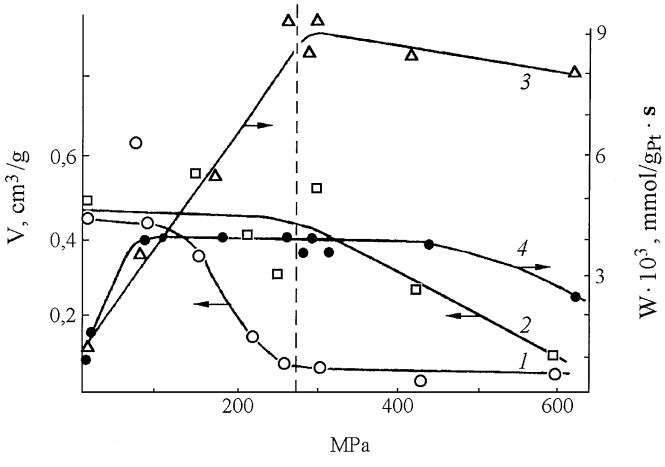

FIG. 10. Influence of molding pressure (2% Pt + γ-Al_2O_3) on the pore volume of molded catalyst (1, pore radius $r > 10$ nm; 2, $r < 10$ nm) and the rate of deep oxidation of n-C_4H_{10} at 300°C (3) and of CH_4 at 500°C (4).

at 300°C (synergy effect). At methane oxidation at 500°C, the activity increases with the growing molding pressure and then attains a plateau when the molding pressure is about 100 MPa. The catalyst obtained under this molding pressure has pore structure similar to that of the initial γ-alumina, which contains large pores with a radius of 10–70 nm. Therefore, the average distance between the particles is 10–70 nm, including that between the platinum and alumina particles. If we support radical traps such as KCl, or CsCl on alumina, and then compress the mechanical mixture of the thus-modified alumina with platinum black, and if the KCl or CsCl concentration on γ-alumina is 1 wt%, the synergy effect between Pt black and γ-Al_2O_3 disappears completely during butane oxidation and is strongly suppressed (approximately by 2-fold) in methane oxidation. Therefore, we may draw the following conclusions:

(1) The synergy effect is related to the transfer of active species (radicals) onto the alumina surface, their accumulation in the pores of alumina, which is inactive as a catalyst, and the development of chain oxidation reactions on the pore surface (since the free flight path of molecules at such a temperature is longer than the diameter of the pores).

(2) The synergy effect dependence on the porous structure of the catalyst pressed into tablets allows one to state that the possible exit of an active radical from its birthplace is about 10–70 nm, which is far less than the roughness of the catalyst surface. Therefore, with no accumulation of radicals (alumina) these radicals are oxidized on the platinum surface to some inactive species before the homogeneous reaction starts.

CONCLUSION

New kinetic data related to the deep oxidation of methane on manganese oxide–alumina and platinum–alumina catalysts are presented. From the results obtained it follows that the more active the catalyst in the deep oxidation of methane, the less the probability for a homogeneous reaction to occur, even at 800°C at various gas mixture compositions including those close to stoichiometry.

An idea for a new method for revealing radicals in chemical reactions on solid catalysts is demonstrated. The distance of the possible exit of active radicals from their birthplace is evaluated.

ACKNOWLEDGMENT

The authors acknowledge the financial support of the Russian Foundation for Basic Research, Project 95-03-08915a.

REFERENCES

1. Gogin, L. L., Matros, Yu. Sh., and Ivanov, A. G., *in* "Ecology and Catalysis," p.107. Nauka, Novosibirsk, 1990.

2. Matros, Yu. Sh., and Bunimovich, G. A., *Catal. Rev. Sci. Eng.* **38**(1), 1 (1996).
3. Tsyrulnikov, P. G., Stuken, S. A., Kudrja, E. N., Balashov, V. A., Kachkina, O. A., Lyubushkin, V. A., and Atamanchuk, O. V., "Catalyst for Deep Oxidation of Carbon Oxide and Organic Compounds," Russian Patent 2063803, July 20, 1996; U.S. Patent 5,880,059, Mar. 9, 1999.
4. Drozdov, V. A., Gogin, L. L., Tsyrulnikov, P. G., and Matros, Yu. Sh., *in* "Unsteady State Processes in Catalysis," International Conference, Book of Abstracts (Yu. Sh. Matros, Ed.), p. 249. Novosibirsk, Russia, 1990.
5. El-Shobaky, G. A., Fagal, G. A., Chozza, A. M., and Shouman, M. A., *Mater. Lett.* **19**, 225 (1994).
6. Tsyrulnikov, P. G., Kovalenko, O. N., Gogin, L. L., Starostina, T. G., Noskov, A. S., Kalinkin, A. V., Krjukova, G. N., Tsybulja, S. V., Kudrja, E. N. and Bubnov, A. V., *Appl. Catal. A Gen.* **167**, 31 (1998).
7. Baltanas, M. G., Stiles, A. V., and Katzer, J. R., *Appl. Catal.* **20**, 31 (1986).
8. Kijlstra, W. S., Roels, E. K., Bliek, A., Weckhuysen, B. M., and Schoonheydt, R. A., *J. Phys. Chem.* B **101**, 309 (1997).
9. Kochubey, D. I., Kriventsov, V. V., Kustova, G. N., Odegova, G. V., Tsyrulnikov, P. G., and Kudrja, E. N., *Kinet. Katal.* **39**(2), 294 (1998).
10. Tsybulja, S. V., Krjukova, G. N., Vlasov, A. A., Boldyreva, N. N., Kovalenko, O. N., and Tsyrulnikov, P. G., *React. Kinet. Catal. Lett.* **64**(1), 11 (1998).
11. Kiperman, S. L., *in* "Kinetics and Catalysis Problems," Vol. 18, p. 14. Nauka, Moscow, 1981 (in Russian).
12. Dryakhlov, A. S., Zhdanovich, N. V., Kisarov, V. M., Kartashov, V. R., Beskov, V. S., and Kiperman, S. L., *Izvenstia AN SSSR, Ser. Khim.* **8**, 1728 (1981).
13. Popovskii, V. V., *Kinet. I Katal.* **10**(5), 1068 (1969); *Kinet. I Katal.* **13**(5), 1190 (1972).
14. Starostina, T. G. Pivovarova., I. V., Tsurylnikov, P. G., and Popovskii, V. V., *J. Appl. Chem.* **53**(5), 1004 (1980).
15. Popovskii, V. V., and Sazonov, V. A., Eds, "Industrial Catalysts for Gas Purification," vyp. 2, p. 37. Novosibirsk, Russia, 1990.
16. Panfilov, N., *Kinet. Catal. (Eng. Trans.)*, **5**, 49 (1964); Ermolaev, V. K., Pak, S. N., Krishtopa, L. G., Ismagilov, Z. R., and Zamaraev, K. I., *Khim. Fiz.* **7**(8), 1141 (1988) (in Russian); Lunsford, J. H., *Langmuir* **5**, 12 (1989).
17. Sal'nikov, V. S., and Tsyrulnikov, P. G., *Kinet. Katal.* **29**, 1117 (1988).
18. Tsyrulnikov, P. G., Sal'nikov, V. S., and Noskov, A. S., *in* "II International Conference. Modern Trends in Chemical Kinetics and Catalysis," Book of Abstracts (V. N. Parmon, Ed.), Part II (2), p. 404. Novosibirsk, Russia, 1995.